Compressive strength of partially stiffened cylinders at elevated temperatures

Egler Araque, Carlos Graciano, David G Zapata-Medina, Octavio Andrés González Estrada

Vol. 19, n.° 1, pp. 131-142, 2020
Revista UIS Ingenierías
Página de la revista: revistas.uis.edu.co/index.php/revistauisingenierias

Compressive strength of partially stiffened cylinders at elevated temperatures

Resistencia a la compresión de cilindros parcialmente rígidos a temperaturas elevadas

Egler Araque [1], Carlos Graciano [2a], David G. Zapata-Medina [2b], Octavio Andrés González-Estrada [3]

[1]Grupo Intevep, S.A., Venezuela. Email: araquee@pdvsa.com
[2] Universidad Nacional de Colombia, Medellín, Colombia. Orcid: [a] 0000-0003-0659-7963, [b] 0000-0001-8868-8740
Emails: [a] cagracianog@unal.edu.co, [b] dgzapata@unal.edu.co
[3]Grupo de Investigación en Energía y Medio Ambiente (Giema), School of Mechanical Engineering, Universidad Industrial de Santander, Colombia. Orcid: 0000-0002-2778-3389. Email: agonzale@uis.edu.co

Received: 26 March 2019. Accepted: 14 October 2019. Final version: 27 December 2019.

Abstract

This work presents the finite element analysis of partially stiffened cylinders subjected to axial compression at elevated temperatures. The compressive strength is calculated for self-weight conditions and the influence of the temperature on the material response is also investigated. In the oil industry, pressure vessels are commonly used operating at complex design conditions such as high-pressure profiles and/or elevated temperature gradients which affect considerably the structural response of inner components. Among them, risers become sensitive steel elements withstanding heavy compressive loading due to self-weight, as well as, insulation elements added to protect them from the elevated temperature gradient. Most risers structurally fail at the bottom end due to buckling caused by self-weight and temperature effects. To remediate this situation and to guarantee the integrity of the riser, longitudinal stiffeners are welded at the bottom end. Hence, a proper determination of the compressive strength of the cylinder, taking into account the influence of the longitudinal stiffening and the corresponding temperature, is required. Results indicate that the use of longitudinal stiffeners in deformed cylinders increases the strength to buckling in percentages that vary according to the cross-section of the profiles.

Keywords: compressive strength; stainless steel; finite element analysis; elevated temperature; longitudinal stiffening.

Resumen

Este trabajo presenta el análisis de elementos finitos de cilindros parcialmente rígidos sometidos a compresión axial a temperaturas elevadas. La resistencia a la compresión se calcula para las condiciones de peso propio y también se investiga la influencia de la temperatura en la respuesta del material. En la industria del petróleo, los recipientes a presión se utilizan comúnmente para operar en condiciones de diseño complejas, como perfiles de alta presión y/o gradientes de temperatura elevados que afectan considerablemente la respuesta estructural de los componentes internos. Entre ellos, los *raisers* se convierten en elementos de acero sensibles que soportan una carga alta de compresión debido al peso propio, así como, elementos de aislamiento agregados para protegerlos del gradiente de temperatura elevada. La mayoría de los *raisers* fallan estructuralmente en el extremo inferior debido a la deformación causada por el peso propio y los efectos de temperatura. Para remediar esta situación y garantizar la integridad de la tubería vertical, los refuerzos longitudinales están soldados en el extremo inferior. Por lo tanto, se requiere una evaluación adecuada de la resistencia a la compresión del cilindro, teniendo en cuenta la influencia del refuerzo

ISSN Printed: 1657 - 4583, ISSN Online: 2145 - 8456, **CC BY-ND 4.0**
How to cite: E. Araque, C. Graciano, D. G. Zapata-Medina, O. A. González-Estrada, "Compressive strength of partially stiffened cylinders at elevated temperatures," *Rev. UIS Ing.*, vol. 19, no. 1, pp. 131-142, 2020. doi: 10.18273/revuin.v19n1-2020013

longitudinal y la temperatura correspondiente. Los resultados indican que el uso de refuerzos longitudinales en cilindros deformados aumenta la resistencia al pandeo en porcentajes que varían de acuerdo con la sección transversal de los perfiles.

Palabras clave: resistencia a compresión; acero inoxidable; análisis de elementos finitos; temperatura elevada; rigidización longitudinal.

1. Introduction

In recent years, in oil refineries, there have been several failure reports regarding the risers in pressure vessels and reactors. These failures are characterized by local deformations at the bottom of the riser (see Figure 1) due mainly to two effects: the self-weight of the structural component combined with a corresponding insulation layer and the elevated operating temperatures.

Thin-walled cylindrical members may undergo local deformations because of local buckling [1]. Timoshenko [2] conducted pioneer works describing the behavior of structural elements under compressive loads. Koiter [3] investigated the influence of initial geometric imperfections on the ultimate strength of thin-walled members. Thereafter, previous studies [4]–[6] used shell theory to investigate the critical buckling load of cylindrical members. Other studies [7]–[10] have dealt with the effect of non-uniform loading and geometric initial shape imperfections. Amazigo [11] varied the size of the initial shape imperfections, Arborcz [12] measured the actual imperfection distribution of stiffened cylindrical shells, and Chryssanthopoulos et al. [13] proposed mathematical models based on regression analyses for these imperfections. Temperature effects were also analyzed by [14]–[16], leading to a closer approximation between experimental values and theoretical predictions for the critical and ultimate loads of cylindrical members.

Figure 1. Typical deformation patterns at the riser bottom. Source: The authors.

It is well known that the compressive strength of structural members can be increased by using longitudinal and inner stiffeners [17]–[19]. When a riser integrity assessment indicates a premature failure, the situation is usually solved by welding longitudinal stiffeners at the bottom. Hence, the riser remains partially stiffened until full replacement. This situation has received little attention in the technical literature. Therefore, this paper presents a numerical investigation of the ultimate compressive strength for partially stiffened cylinders. The research is conducted in two stages. One dealing with linear buckling analysis to investigate the effect of the initial geometric imperfections (shape and size). This methodology is validated with analytical formulas available in the literature. A second stage deals with the nonlinear finite element analysis of the stiffened cylinder taking into account both initial imperfection and temperature effects on the elastoplastic behavior of the material [20]. The results show the enhancing effect of the stiffeners on the compressive strength of the risers and the detrimental effect on the buckling resistance of initial imperfections and high temperatures.

2. Eigenvalue analysis

In order to model the initial shape imperfections, a linear eigenvalue analysis is performed to obtain the critical buckling loads and corresponding buckling modes [18], [21]. The analysis is conducted using the Finite Element (FE) software ABAQUS [22]. Shell elements S9R5 from the ABAQUS element library were used to model cylindrical members. This element type was also used by [23]–[25], among others, they have five degrees of freedom (three displacement components and two in-surface rotation components), and is an economical shell element recommended for thin bodies and buckling. Figure 2 shows a schematic view of the cylinder element considered in this work.

Figure 3 presents the numerical model and illustrates the boundary conditions employed. In order to introduce the self-weight of the component, an equivalent body load q=13,286 kg/m^3, acting in the longitudinal direction, is considered. Regarding boundary constraints, all six degrees of freedom at the bottom of the cylinder were restricted, representing a fully fixed condition.

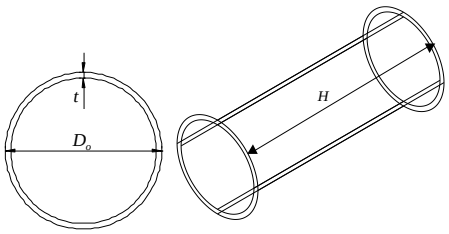

Figure 2. Geometry of the cylinders. Source: The authors.

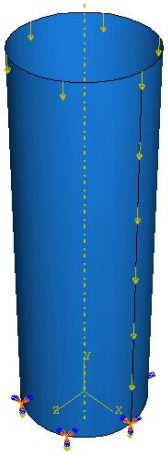

Figure 3. Applied loads and boundary conditions. Source: The authors.

Table 1 lists the models and geometries used in the analysis, where t is the thickness, D_0 is the diameter, and H is the height. A total of 12 models are included. These models cover most riser geometries used in the oil refinery industry. For each geometry, the first three buckling modes are calculated, while only the critical buckling stress for the first mode is determined.

Table 1. Geometrical dimensions of the models used in the parametric analysis

Model	t (mm)	D_o (mm)	H (mm)	D_o/t	H/D_o
1	6.35	1270	1270	200	1
2	6.35	1270	2540		2
3	6.35	1270	3810		3
4	6.35	1270	5080		4
5	12.70	3810	3810	300	1
6	12.70	3810	7620		2
7	12.70	3810	11430		3
8	12.70	3810	15240		4
9	25.4	5080	5080	400	1
10	25.4	5080	10160		2
11	25.4	5080	15240		3
12	25.4	5080	20320		4

Seung and Chang [23] proposed Eq. (1) to estimate the buckling stress of cylindrical members. Table 2 shows a comparison between the critical buckling stress calculated with Eq. (1), and the computed results obtained using the numerical model. Numerical results show good agreement with those obtained using Eq. (1) with a maximum difference of approximately 2%. Theoretical predictions were calculated assuming a Young's modulus E = 140 GPa, adjusted based on a temperature of 704 °C (see Table 3). For the FE models, a Poisson's ratio, ν, of 0.3 and an equivalent mass density, ρ, of 13286 kg/m^3, considering the steel and insulation layer of the member, were used.

$$\frac{\sigma_{cr}}{E} = 1.28\left(\frac{H}{D_0}\right)^{-0.0256}\frac{t}{D_0} \quad (1)$$

Table 2. Comparison between theoretical and computed critical stresses

Model	σ_{cr} Eq.(1) (MPa) (a)	σ_{cr} FEM (MPa) (b)	(a)/(b)
1	832.69	849.00	1.01
2	818.05	845.48	1.03
3	809.60	818.01	1.01
4	803.66	802.79	1.00
5	555.13	561.67	1.01
6	545.36	558.31	1.02
7	539.73	540.13	1.00
8	535.77	532.02	0.99
9	416.34	419.07	1.01
10	409.02	412.44	1.01
11	404.80	402.56	0.99
12	401.83	397.07	0.99

Table 3. Elastic moduli for a steel ASTM 240 type 304H

Young's modulus	Temperature (ºC)					
	538	593	649	704	760	816
1×10^6 psi	22.8	22	21.2	20.3	19.2	18.1
1×10^9 Pa	157	151	146	140	132	125

Source: ASME Code Section II Part D [26].

The deformations obtained from the buckling modes are normalized using the ratio between the displacement of each node and the maximum nodal displacement. Figure 4 shows the shape of the first three buckling modes for Model 5, reported in Table 1. The estimates of the eigenvalues and the first three buckling modes for the 12 models proposed are given by the convergence presented by the mesh for each one of them. In the models the number of nodes arranged circumferentially and longitudinally was increased, considering the results

presented by [23], [25], according to which the load and buckling mode obtained by the numerical model for thin-wall cylinders are affected to a greater degree by the number of finite elements arranged in the circumferential direction.

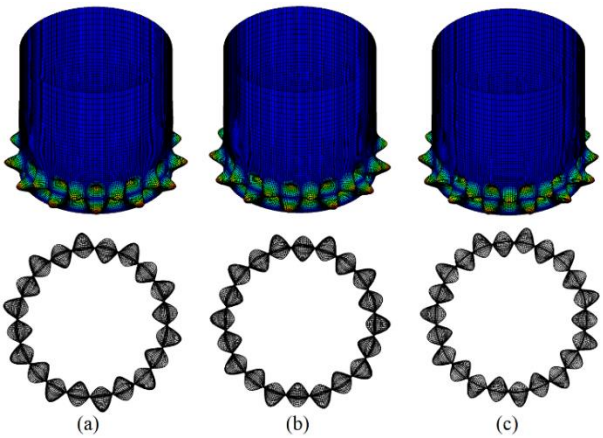

Figure 4. Buckling modes for Model 5 (D_o/t =300; H/D_o =1): a) 1st mode, b) 2nd mode, and c) 3rd mode. Source: The authors.

3. Ultimate strength analysis

3.1. Elastoplastic material behavior

The stress-strain behavior for most metals is described by the Ramberg-Osgood [27] relationship, which describes stress as an implicit function of total deformation. It has been established that for levels below the value of the yield stress, this function is highly consistent with the results obtained experimentally. However, for stress levels above the yield stress, the ratio tends to overestimate such stress.

Recently, [28], [29] proposed a modification of the Ramberg-Osgood version, which significantly improves the prediction of the experimental behavior of the stress-strain curve for the whole range of stresses.

In this research, the behavior of the stress-strain curve for the ASTM 240 type 304H material is defined using the relationships established by [29]. To develop the deformation curves, the yield, S_y and ultimate, S_u, stresses are required, as well as their corresponding strains. With these material properties, a number of constants are determined that are then substituted in the main equation that defines the elastic and plastic behavior of the material.

Table 4 shows the properties required to define the behavior of a steel ASTM 240 type 304H. These properties are given in the Stainless Steels Handbook (1996).

Table 4. Yield and ultimate stress and strain for ASTM type 240 304H

Temperature T (ºC)	**Yield stress S_y (MPa)**	**Ultimate stress S_u (MPa)**	**Ultimate strain ε_u**
537.78	265.46	427.49	0.41
648.89	213.75	324.07	0.58
760.00	162.03	206.85	0.46
871.11	112.39	118.59	0.48

The relationships established by [29] are described as follows:

$$e = \frac{S_y}{E} \tag{2}$$

$$n = \frac{1}{0.0375}\left[1 - \frac{S_u}{S_y}(0.2 + 185e) + 5\right] \tag{3}$$

$$\varepsilon_{0.2} = \frac{S_y}{E} + 0.002 \tag{4}$$

$$r = E\frac{\varepsilon_{0.2}}{S_y} \tag{5}$$

$$E_2 = \frac{E}{1 + 0.002n/e} \tag{6}$$

$$r_2 = E_2\frac{\varepsilon_{0.2}}{S_y} \tag{7}$$

$$p = r\frac{(1 - r_2)}{(r - 1)} \tag{8}$$

$$\varepsilon_{nu} = \frac{\varepsilon_u}{\varepsilon_{0.2}} \tag{9}$$

$$r^* = E_2\frac{(\varepsilon_u - \varepsilon_{0.2})}{(S_u - S_y)} \tag{10}$$

$$m = 1 + 3.5\frac{S_y}{S_u} \tag{11}$$

$$E_u = \frac{E_2}{1 + (r^* - 1)m} \tag{12}$$

$$r_u = E_u\frac{(\varepsilon_u - \varepsilon_{0.2})}{(S_u - S_y)} \tag{13}$$

$$p^* = r^*\frac{(1 - r_u)}{(r^* - 1)} \tag{14}$$

$$S_n = \begin{cases} \dfrac{r\varepsilon_n}{1+(r-1)\varepsilon_n^p} & 0 \le \varepsilon_n \le 1 \\ 1+\dfrac{r_2(\varepsilon_n-1)}{1+(r^*-1)\left(\dfrac{\varepsilon_n-1}{\varepsilon_{nu}-1}\right)^{p*}} & 1 \le \varepsilon_n \le \varepsilon_{nu} \end{cases} \quad (15)$$

$$S_n = \frac{S_i}{S_y} \quad (16)$$

where n represents a non-linearity index, e is a non-dimensional proof stress, $\varepsilon_{0.2}$ is the total strain corresponding to the 0.2% proof stress, E_2 is the tangent modulus, E_u is the slope of the full-range stress-strain at $\varepsilon = \varepsilon_{nu}$, S_n is the normalized stress.

Employing Eqs. (2)-(16) and taking the properties of Table 4, the curves shown in Figure 5 were constructed for a steel ASTM 240 type 304H, working within a temperature range equal to 540°C ≤ T ≤ 815°C.

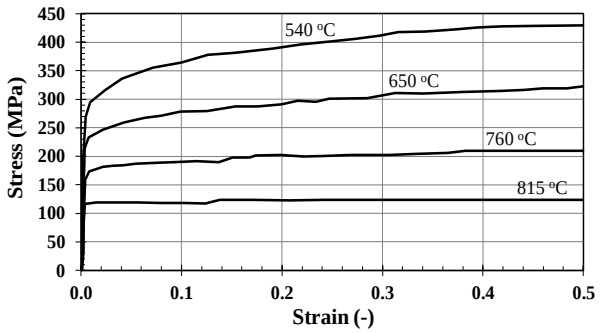

Figure 5. Elastoplastic behavior of a steel ASTM 240-304H under various temperatures.

3.2. Geometrical model

In this section, a nonlinear finite element analysis is conducted using the same element (i.e., S9R5) as used in the eigenvalue analysis. Initial shape imperfections were modeled with the first buckling mode obtained previously, and the maximum amplitude was normalized. Basically, the geometries are the same as reported in Table 1. For the calculations of the ultimate strength, the density of the cylinders was considered as 13286 kg/m^3. It is significantly greater than the corresponding value for the steel due to the addition of an insulation layer, which does not contribute to the stiffness of the cylinder. In engineering practice, the cylindrical risers are stiffened only at the bottom. In a similar manner, the cylinders investigated herein were stiffened at only 10% of their total height. Figure 6 shows three representative deformed configurations for Model 7: unstiffened in Figure 6a, partially stiffened with ten stiffeners in Figure 6b, and stiffened with 20 stiffeners in Figure 6c. Figure 7 and Table 5 shows the geometry and dimensions, respectively, of the profiles used to stiffen the risers. The nonlinear finite element analysis was performed using the modified arc-length method [30] to properly trace the path of the load-displacement response of the cylinders.

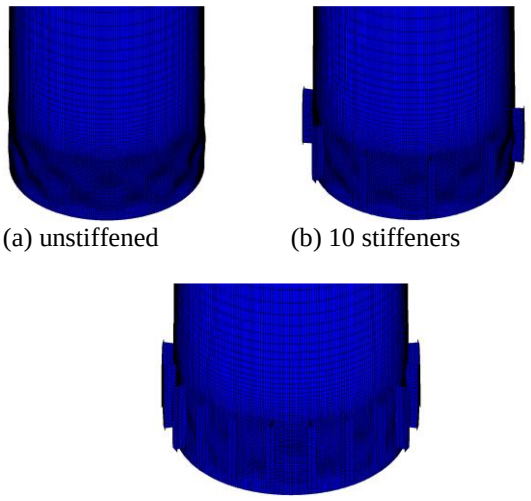

(a) unstiffened (b) 10 stiffeners

(b) 20 stiffeners

Figure 6. FEM model for the cylinders using the 1st buckling mode (Model 7).

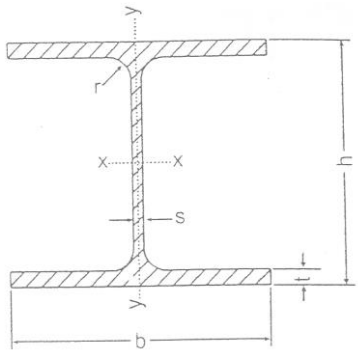

Figure 7. Profile HEA according to DIN 1025. (ASTM A – 6).

Table 5. Dimensions of the HEA profiles

Profile	*h* (mm)	*b* (mm)	*t* (mm)	*s* (mm)	*r* (mm)
100	96	100	8.0	5	12
120	114	120	8.0	5	12
140	133	140	8.5	5.5	12
160	152	160	9.0	6	15
180	171	180	9.5	6	15
200	190	200	10.0	6.5	18
220	210	220	11.0	7	18

3.3. Model validation

To evaluate the effect of the geometry of the stiffener element on the final buckling load, seven stiffened

cylinders with ten profiles were constructed from the geometry of the Model 8 defined in Table 1, considering the dimensions of the seven profiles presented in Table 5. The main reason for the selection of Model 8 is the fact that it corresponds to the geometric conditions of the riser of El Palito Refinery, which is the unit that has presented the most problems of localized deformation. Additionally, a geometric disturbance was included for the first buckling mode, equivalent to 0.025 m (1 in) of deformation in the radial direction.

Another aspect evaluated in the stiffened cylinders is the variation of the initial deformation present in the structures, considering the deformation of the cylinder as a perturbation of the geometry, which was included in the models through the first buckling mode. This sensitivity analysis was carried out for the Model 8 to determine the influence of the initial deformations on the ultimate load of the stiffened cylinders. The study was limited to a configuration of 10 profiles of type HEA 220 (see Table 5) distributed in a uniform manner.

Finally, with the numerical models defined, the influence of the temperature was evaluated by changing the mechanical properties of the ASTM 240 type 304H material. The considered temperature range corresponds to 593°C ≤ T ≤ 816°C.

Figure 8 shows the convergence analysis according to the critical buckling load and the maximum von Mises stress for Model 8. This analysis was conducted for the 12 models described in Table 1. The mesh for each one of the models proposed in the parametric study was obtained through a convergence analysis. For mesh independence, several meshes were solved on each model in order to determine the load and buckling mode. The meshes were modified until the load, mode, and strain energy parameters showed small variation.

4. Parametric analysis

In this section, a sensitivity study is conducted considering the effects of:

- Amplitude of the initial geometric imperfection.
- Size and amount of profiles.
- Shape of the geometric imperfections on the compressive strength of the cylinders.
- Temperature.

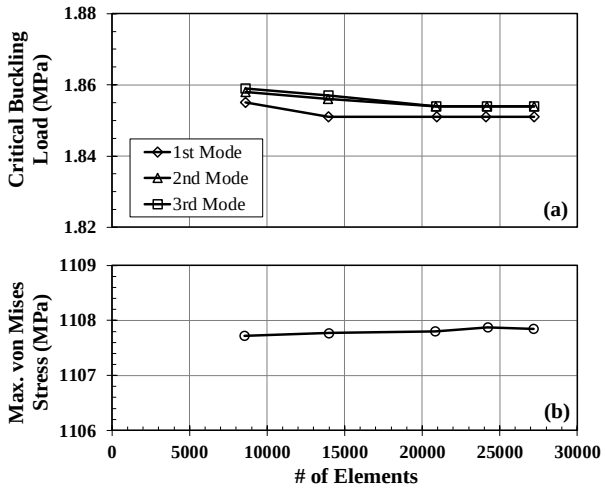

Figure 8. (a) Critical buckling load and (b) maximum von Mises stress for Model 8.

4.1. Effect of the amplitude of the initial imperfection

The effect of varying the amplitude of the deformation on the ultimate load in cylindrical structures stiffened with commercial profiles was evaluated in Model 8. A range of initial deformation comprised between 6.35mm≤w_o≤50.80mm in 6.35mm intervals was considered, starting from a uniform configuration of 10 profiles. In Figure 9 we represent the results for the normalized ultimate load ($\frac{q}{q_c}$) vs. the displacement. It is observed that the behavior of the curves is very similar, that is, they are linear in the first place and as the load increases, the vertical displacements also increase until each one reaches the collapse load or ultimate load. After that point, the load begins to decrease while the displacement continues to increase. It is appreciated that in each curve the cylinder maintains some load capacity in the zone after the ultimate load. This load capacity decreases as the size of the initial deformation increases.

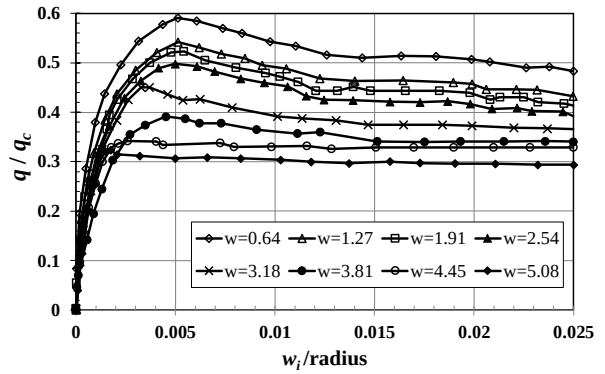

Figure 9. Load-displacement responses for various imperfection amplitudes.

The results presented in Figure 9 agree with the studies by [12], in the sense that small perturbations in the geometry of the cylinders significantly impact the ultimate load. Arbocz [12] found that for amplitudes of imperfections that are on the order of a relative magnitude w/t = 4, the ultimate load reaches 39% of the theoretical load (load for a cylinder with perfect geometry). For the case under study, it was obtained that for an initial deformation of 5.08 cm (2 inches), with w/t = 4, the ultimate load decreases to 30% of the theoretical load (Table 6) Unlike the research carried out by [12], which considers that the stiffener web maintains its constant shape despite the initial deformations of the cylinders, this study considered that the web of the stiffening elements is modified such that the stiffener surface adapts to the deformed cylindrical surface. In this way, the model considers common practices performed during the repair process of the risers in the regenerative reactors of the refineries in Venezuela.

Table 6. Influence of the initial deformations on the ultimate load

Deformation w (cm)	$\frac{q}{q_c}$
0.64	0.59
1.27	0.54
1.91	0.52
2.54	0.49
3.18	0.45
3.81	0.39
4.45	0.32
5.08	0.3

4.2. Effect of the size of the profiles

The effect of the geometry of the stiffeners is evaluated in Model 8 (Figure 10). We consider seven commercial profiles type HEA and measure the effect on the ultimate buckling load. We use a uniform configuration of 10 profiles and an initial deformation of 2.54 cm (1 in) (Figure 10b).

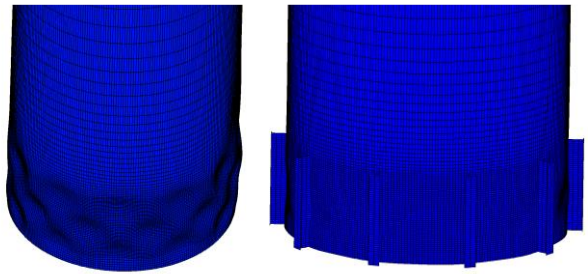

(a) without stiffeners (b) with 10 HEA 180 stiffeners

Figure 10. First buckling mode for Model 8

Figure 11 shows the results of the normalized buckling load vs. displacement for the HEA profiles. The results obtained indicate that the use of HEA type commercial profiles increases the ultimate load on deformed cylinders: For the case of Model 8, 49% of the theoretical load is required to reach the ultimate load on the unstiffened cylinder (Table 7). By adding the longitudinal stiffeners to the deformed model, an increase of up to 28.57% in the final buckling load is obtained when using HEA 220 type profiles (Table 7).

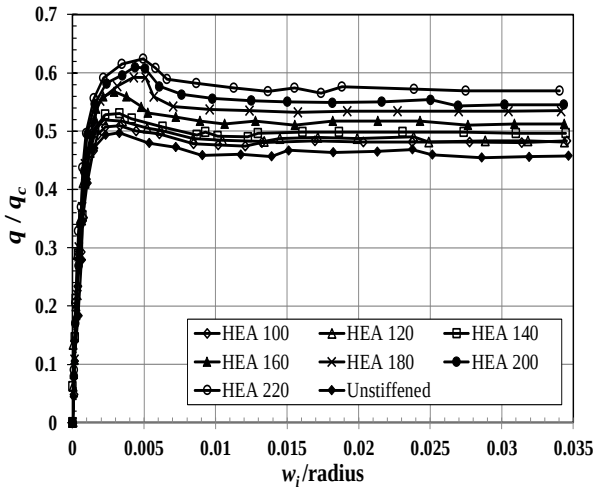

Figure 11. Effect of the HEA stiffeners on the ultimate buckling load.

Table 7. Ultimate buckling load in stiffened cylinders with commercial profiles type HEA

HEA profile	$\frac{q}{q_c}$	**% load increment**
Unstiffened	0.49	0
100	0.51	4.08
120	0.52	6.12
140	0.53	8.16
160	0.57	16.32
180	0.59	20.80
200	0.6	22.44
220	0.63	28.57

From Table 7 we can conclude that the use of longitudinal stiffeners requires a careful selection of the dimensions of the profile to be used. Both the load requirements of the structure and the condition of the material must be taken into account, since the stiffening effect of some profiles can be overestimated. An example of this argument is represented by the small increase of 4% in the ultimate load of a riser that presents an initial deformation of 0.025 m (1 inch) and that is stiffened by 10 profiles type HEA 100.

4.3. Effect of the number of the stiffener profiles

Stiffening of the riser using profiles has been done so far considering only the degree of deformation of the structures and the geometry of the profiles. In this section, we study the influence of the number of profiles on the final buckling load on deformed and stiffened cylinders. Figure 12 shows the normalized ultimate buckling load for Model 8 stiffened by 5, 10, 15 and 20 commercial profiles type HEA 160.

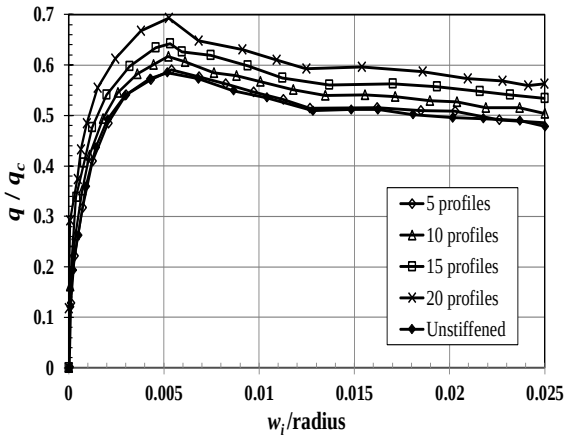

Figure 12. Influence of the number of profiles on the ultimate buckling load of Model 8.

Table 8. Influence of the number of commercial profiles on the ultimate buckling load of Model 8

Number of profiles	$\frac{q}{q_c}$	% load increment
Unstiffened	0.56	0
5	0.57	1.79
10	0.59	5.35
15	0.62	10.71
20	0.68	21.43

The results shown in Figure 12 and Table 8 indicate that the ultimate load for stiffened cylinders highly depends on the number of structural elements used to increase their stiffness. Placing 5 profiles increases the ultimate buckling load by 1.79%, while 20 profiles increase the ultimate buckling load by 21.43%.

4.4. Effect of the buckling mode

The effect of the shape of the initial geometrical defect in the ultimate buckling load of stiffened cylinders is investigated, maintaining a constant amplitude of the deformation of one inch. We consider the stiffened models with 10 and 20 profiles type HEA 180, with imperfections resulting from the first three buckling modes of the structures, as shown in Figure 13.

The effect of varying the shape of the initial imperfections present in the stiffened cylinders is shown for the first three buckling modes in Figure 14.

The curves obtained for the cylinders with and without stiffeners present a very similar response. Each curve describes a linear behavior and, as the load increases, the displacement increases until reaching the ultimate buckling load. The ultimate load values for the different buckling modes of Model 4 and Model 11 are shown in Table 9 and Table 10. The results indicate that the first buckling mode does not necessarily induce the lowest ultimate load on the cylindrical structure. From the 12 cases analyzed, the third buckling mode leads to obtaining the lowest ultimate buckling load in models 4, 6 and 9.

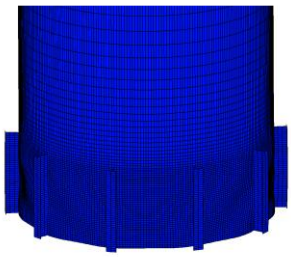

(a) 10 stiffeners.

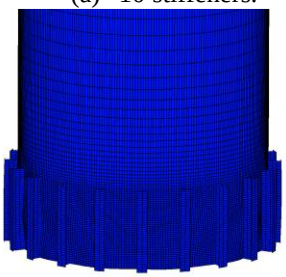

(b) 20 stiffeners.

Figure 13. Shape mode for model 8.

Table 9. Normalized ultimate buckling load $\frac{q}{q_c}$ for Model 4

Buckling mode	Unstiffened	10 profiles	20 profiles
1	0.2	0.38	0.59
2	0.19	0.3	0.5
3	0.21	0.25	0.43

Table 10. Normalized ultimate buckling load $\frac{q}{q_c}$ for Model 11

Buckling mode	Unstiffened	10 profiles	20 profiles
1	0.47	0.38	0.5
2	0.39	0.43	0.49
3	0.42	0.49	0.53

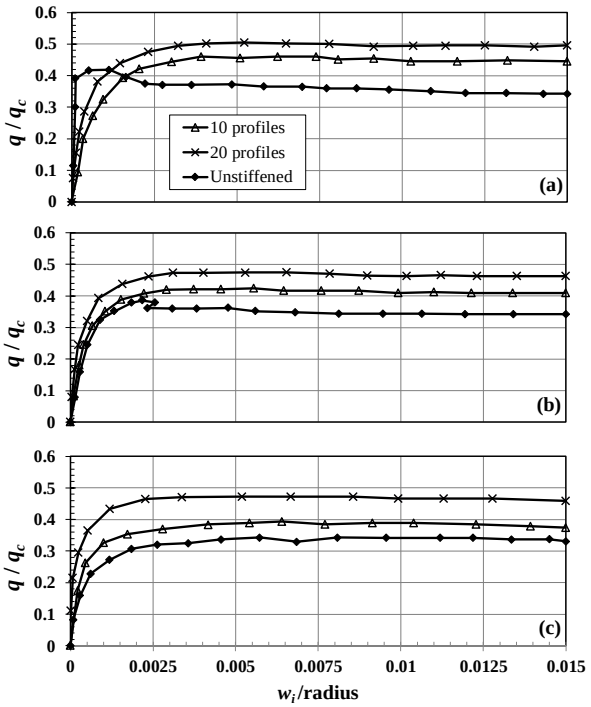

Figure 14. Ultimate buckling load for model 10: (a) Mode 1; (b) Mode 2; and (c) Mode 3.

In Table 11 we compare the results of the ultimate load for Model 12. It is observed that for a certain number of profiles, the longitudinal stiffeners provide different levels of increase of the ultimate load, by varying the shape of the geometric imperfection in the cylinders. For the case of model 12, with an initial deformation of 0.025 m (1 in), stiffening the cylinder with 10 profiles increases the ultimate load in a range of 4.76% to 12.5%, while for the alternative of the 20 profiles, this load rises between 32.43% to 45%. These increments of the ultimate load depend on the buckling mode that is considered as imperfection.

Table 11. Normalized ultimate buckling load $\frac{q}{q_c}$ for Model 12

Buckling mode	Unstiffened	10 profiles	% increment	20 profiles	% increment
1	0.42	0.44	4.76	0.6	42.86
2	0.4	0.45	12.5	0.58	45
3	0.37	0.41	10.81	0.49	32.43

4.5. Effect of the temperature

The effect of temperature was studied by varying the modulus of elasticity and the stress-strain curve. The evaluation was made from the analytical models developed for the nonlinear analysis, adjusting the properties according to the temperature that was being considered. A compendium of these results is shown in Table 12. It is observed that, in general, each of the curves presents a similar behavior, that is, as the temperature increases, the ultimate buckling load is reduced. This reduction occurs in accordance with the decrease in the modulus of elasticity of the ASTM 240 type 304H material.

Table 13 shows the percentage of decrease in the ultimate buckling load for different temperatures. It can be observed that the variation of the ultimate load with respect to temperature is within a very specific range, so for a temperature increase of 593 ºC to 649 ºC the ultimate load decreases within 1, 92% to 4.35%, from 593 ºC to 704 ºC within 4% to 6.52%, from 593 °C to 760 °C within 8% to 10.87%, finally, if the temperature of the material changes from 593 °C at 816 °C the decrease is within 12% to 17.39%.

Table 12. Influence of temperature on the ultimate buckling load $\frac{q}{q_c}$

Model	593 ºC	649 ºC	704 ºC	760 ºC	816 ºC
1	0.48	0.47	0.46	0.44	0.41
2	0.47	0.46	0.45	0.43	0.4
3	0.45	0.44	0.43	0.41	0.39
4	0.44	0.43	0.42	0.4	0.38
5	0.52	0.51	0.49	0.47	0.44
6	0.5	0.49	0.48	0.46	0.44
7	0.49	0.48	0.47	0.45	0.43
8	0.48	0.47	0.45	0.43	0.4
9	0.48	0.47	0.46	0.44	0.41
10	0.46	0.45	0.44	0.42	0.39
11	0.46	0.44	0.43	0.41	0.38
12	0.44	0.43	0.42	0.4	0.38

Table 13. Percentage of decrease in the ultimate load $\frac{q}{q_c}$

Model	649 ºC	704 ºC	760 ºC	816 ºC
1	2.08	4.17	8.33	14.58
2	2.13	4.26	8.51	14.89
3	2.22	4.44	8.89	13.33
4	2.27	4.55	9.09	13.64
5	1.92	5.77	9.62	15.38
6	2.00	4.00	8.00	12.00
7	2.04	4.08	8.16	12.24
8	2.08	6.25	10.42	16.67
9	2.08	4.17	8.33	14.58
10	2.17	4.35	8.70	15.22
11	4.35	6.52	10.87	17.39
12	2.27	4.55	9.09	13.64

5. Conclusions

In the present work, we studied the behavior of buckling in risers subjected to axial compression. We studied a series of parameters that can be used as a reference for the selection of profiles to stiffen a cylindrical structure. The risers were considered as a thin-walled cylindrical element with initial imperfections that presented different shapes and amplitudes. The methodology used was to determine, by linear analysis, the load and shape of the first three buckling modes of the structures. Then, these modes were used as geometric imperfections in a nonlinear analysis for the study of the ultimate strength of cylinders stiffened under different configurations. Finally, the effect of the temperature in the elastoplastic properties of the material ASTM 240 type 304H was studied. The deformations found in the risers allow establishing measures to increase the strength of the cylindrical elements. Based on the presented analyses and results, the following conclusions can be drawn:

- When imperfections are modeled in the form of buckling modes for cylinders, with geometric relationships between $200 \leq \frac{D_o}{t} \leq 400$ and $1 \leq \frac{H}{D_o} \leq 4$, the elements exhibit a typical behavior. They are linear at first and, as the load increases, the vertical displacements also increase until each one reaches the ultimate load. This ultimate load is significantly influenced by the buckling mode. For the first three buckling modes, the ultimate load varies by up to 25%. It was determined that the first buckling mode does not necessarily produce the greatest decrease in the ultimate load.
- The amplitude of the deformation significantly affects the ultimate load on stiffened cylinders. For amplitudes between $6.35\ \text{mm} \leq w \leq 50.80\ \text{mm}$ a decrease in the ultimate load was found within 8.5% to 46%. The increase of these initial deformations produced a significant decrease in the post-ultimate load capacity in the cylindrical elements with imperfections greater than 0.045 m.
- The use of longitudinal stiffeners in deformed cylinders increases the strength to buckling in percentages that vary according to the cross-section of the profiles. We obtained an increase in the ultimate load from 4%, for the smallest profile (HEA type 100), to 29%, for the larger profile (HEA type 220).
- The ultimate load of stiffened cylinders is significantly influenced by the number of structural elements used. The results indicate that when the number of longitudinal stiffeners is not enough, increments of only 1.79% are obtained, while for other cases, the ultimate load increased up to 21.43%.
- By varying the temperature of the ASTM 240 type 304H material within the temperature range 593 ºC $\leq T \leq$ 816 ºC, we observed a reduction in the ultimate buckling load. This reduction is in agreement with the decrease of the modulus of elasticity of the material. We observed a percent decrease up to 17.39% when reaching 816 ºC.
- The values obtained for the different parameters can be used as guides during the repairs in the unscheduled stops of the risers in the oil refinery industry. The presented results have a wide range of applicability since they consider various geometries and temperatures of the material. It is expected that these results can translate into significant savings in repair time, which is important considering that an oil refinery can process between 25,000 to 40,000 barrels of gasoline per day.

References

[1] L. Friedrich, T.-A. Schmid-Fuertes, and K.-U. Schröder, "Comparison of theoretical approaches to account for geometrical imperfections of unstiffened isotropic thin walled cylindrical shell structures under axial compression," *Thin-Walled Struct.*, vol. 92, pp. 1–9, Jul. 2015, doi:10.1016/j.tws.2015.02.019.

[2] S. Timoshenko, *Theory of elastic stability*. New York: McGraw Hill, 1910.

[3] W. Koiter, "On the stability of elastic equilibrium," University of Delf, 1945.

[4] B. Budiansky and J. W. Hutchinson, "Dynamic buckling of imperfection-sensitive structures," in *Applied Mechanics*, Berlin, Heidelberg: Springer Berlin Heidelberg, 1966, pp. 636–651.

[5] J. M. T. Thompson and G. W. Hunt, *A general theory of elastic stability*. London: Wiley, 1973.

[6] A. B. Brush D, *Buckling of Bars, Plates and Shells*. New York: McGraw-Hill, 1975.

[7] J. Arbocz, "Post-buckling behaviour of structures numerical techniques for more complicated structures," in *Buckling and Post-Buckling*, Berlin/Heidelberg: Springer-Verlag, 1987, pp. 83–142.

[8] X. Ding, R. Coleman, and J. M. Rotter, "Technique for Precise Measurement of Large-Scale Silos and Tanks," *J. Surv. Eng.*, vol. 122, no. 1, pp. 14–25, 1996, doi:10.1061/(asce)0733-9453(1996)122:1(14).

[9] M. Pircher and R. Bridge, "The influence of circumferential weld-induced imperfections on the buckling of silos and tanks," *J. Constr. Steel Res.*, vol.

57, no. 5, pp. 569–580, May 2001, doi:10.1016/S0143-974X(00)00027-4.

[10] F. Mahboubi Nasrekani and H. Eipakchi, "Axisymmetric Buckling of Cylindrical Shells with Nonuniform Thickness and Initial Imperfection," *Int. J. Steel Struct.*, pp. 1–11, Aug. 2018, doi:10.1007/s13296-018-0132-9.

[11] J. C. Amazigo, "Buckling of Stochastically Imperfect Structures," in *Buckling of Structures*, Berlin, Heidelberg: Springer Berlin Heidelberg, 1976, pp. 172–182.

[12] J. Arbocz, "The Imperfection Data Bank, a Mean to Obtain Realistic Buckling Loads," in *Buckling of Shells*, Berlin, Heidelberg: Springer Berlin Heidelberg, 1982, pp. 535–567.

[13] M. K. Chryssanthopoulos, M. J. Baker, and P. J. Dowling, "Imperfection Modeling for Buckling Analysis of Stiffened Cylinders," *J. Struct. Eng.*, vol. 117, no. 7, pp. 1998–2017, 1991, doi:10.1061/(asce)0733-9445(1991)117:7(1998).

[14] L.-W. Chen and L.-Y. Chen, "Thermal postbuckling analysis of laminated composite plates by the finite element method," *Compos. Struct.*, vol. 12, no. 4, pp. 257–270, Jan. 1989, doi:10.1016/0263-8223(89)90075-5.

[15] C. A. Meyers and M. W. Hyer, "Thermal buckling and postbuckling of symmetrically laminated composite plates," *J. Therm. Stress.*, vol. 14, no. 4, pp. 519–540, Oct. 1991, doi:10.1080/01495739108927083.

[16] H.-S. Shen, "Thermal postbuckling analysis of imperfect stiffened laminated cylindrical shells," *Int. J. Non. Linear. Mech.*, vol. 32, no. 2, pp. 259–275, Mar. 1997, doi:10.1016/S0020-7462(96)00054-6.

[17] M. J. Lewandowski, M. Gajewski, and M. Gizejowski, "Numerical analysis of influence of intermediate stiffeners setting on the stability behaviour of thin-walled steel tank shell," *Thin-Walled Struct.*, vol. 90, pp. 119–127, May 2015, doi:10.1016/j.tws.2015.01.019.

[18] Q.-V. Vu, V.-H. Truong, G. Papazafeiropoulos, C. Graciano, and S.-E. Kim, "Bend-buckling strength of steel plates with multiple longitudinal stiffeners," *J. Constr. Steel Res.*, vol. 158, pp. 41–52, Jul. 2019, doi:10.1016/j.jcsr.2019.03.006.

[19] J. D. Argüello-Bastos, C. A. Ruiz-Florián, O. A. González-Estrada, A. D. Pertuz-Comas, and A. Martínez-Amariz, "Compression tests performed in reinforced rigid matrix composite varying the reinforcement material," *J. Phys. Conf. Ser.*, vol. 1126, p. 012007, Nov. 2018, doi:10.1088/1742-6596/1126/1/012007.

[20] J. Martínez, E. Casanova, C. Graciano, and O. A. González-Estrada, "Sensitivity analysis of a member under compression via Monte Carlo method," *Rev. UIS Ing.*, vol. 17, no. 2, pp. 179–184, 2018.

[21] A. Ayestarán, C. Graciano, and O. A. González-Estrada, "Resistencia de vigas esbeltas de acero inoxidable bajo cargas concentradas mediante análisis por elementos finitos," *Rev. UIS Ing.*, vol. 16, no. 2, pp. 61–70, Sep. 2017, doi:10.18273/revuin.v16n2-2017006.

[22] ABAQUS, *ABAQUS/standard user's manual, v.6.9*. Pawtucket, Rhode Island: Hibbitt, Karlsson & Sorensen, Inc., 2009.

[23] S.-E. Kim and C.-S. Kim, "Buckling strength of the cylindrical shell and tank subjected to axially compressive loads," *Thin-Walled Struct.*, vol. 40, no. 4, pp. 329–353, Apr. 2002, doi:10.1016/S0263-8231(01)00066-0.

[24] Y. Song, "Buckling of shells under non-uniform stress states," Hong Kong Polytechnic University, 2002.

[25] C. Y. Song, J. G. Teng, and J. M. Rotter, "Imperfection sensitivity of thin elastic cylindrical shells subject to partial axial compression," *Int. J. Solids Struct.*, vol. 41, no. 24–25, pp. 7155–7180, Dec. 2004, doi:10.1016/j.ijsolstr.2004.05.040.

[26] ASME BPVC.II.D, *Materials, Part D, Properties*. New York: ASME, 2015.

[27] W. Ramberg and W. Osgood, "Determination of stress-strain curves by three parameters. Technical Note No 503," 1941.

[28] E. Mirambell and E. Real, "On the calculation of deflections in structural stainless steel beams: an experimental and numerical investigation," *J. Constr. Steel Res.*, vol. 54, no. 1, pp. 109–133, Apr. 2000, doi:10.1016/S0143-974X(99)00051-6.

[29] K. Abdella, "Inversion of a full-range stress–strain relation for stainless steel alloys," *Int. J. Non. Linear. Mech.*, vol. 41, no. 3, pp. 456–463, Apr. 2006,

doi:10.1016/j.ijnonlinmec.2005.10.002.

[30] E. Riks, “An incremental approach to the solution of snapping and buckling problems,” *Int. J. Solids Struct.*, vol. 15, no. 7, pp. 529–551, 1979, doi:10.1016/0020-7683(79)90081-7.